

**This item is the archived peer-reviewed author-version of:**

Electrochemical evidence for neuroglobin activity on NO at physiological concentrations

**Reference:**

Trashin Stanislav, De Jong Mats, Luyckx Evi, Dewilde Sylvia, De Wael Karolien.- Electrochemical evidence for neuroglobin activity on NO at physiological concentrations

Journal of biological chemistry - ISSN 0021-9258 - (2016), p. 1-18

Full text (Publishers DOI): <http://dx.doi.org/doi:10.1074/jbc.M116.730176>

To cite this reference: <http://hdl.handle.net/10067/1343400151162165141>

## Electrochemical evidence for neuroglobin activity on NO at physiological concentrations

Stanislav Trashin<sup>†</sup>, Mats de Jong<sup>†</sup>, Evi Luyckx<sup>§</sup>, Sylvia Dewilde<sup>§</sup> and Karolien De Wael<sup>†</sup>

From the Departments of <sup>†</sup>Chemistry and <sup>§</sup>Biomedical Sciences, University of Antwerp,  
2010 Antwerp, Belgium

Running title: NGB electro-re-reduction in the presence of NO and O<sub>2</sub>

To whom correspondence should be addressed: Prof. Karolien De Wael, AXES research group, Department of Chemistry, the University of Antwerp, Groenenborgerlaan 171, B-2010 Antwerp, Belgium. Telephone: (32) 3-265-3335, E-mail: [karolien.dewael@uantwerpen.be](mailto:karolien.dewael@uantwerpen.be)

**Keywords:** neuroglobin, nitric oxide, oxygen, electrochemistry

---

### ABSTRACT

The true function of neuroglobin (Ngb) and, particularly, human NGB (NGB) has been under debate since its discovery 15 years ago. It has been expected to play a role in oxygen binding/supply, but a variety of other functions have been put forward, including NO dioxygenase activity. However, *in vitro* studies that could unravel these potential roles have been hampered by the lack of an Ngb-specific reductase. In this work, we used electrochemical measurements to investigate the role of an intermittent internal disulfide bridge in determining NO oxidation kinetics at physiological NO concentrations. The use of a polarized electrode to efficiently interconvert the ferric (Fe<sup>3+</sup>) and ferrous (Fe<sup>2+</sup>) forms of an immobilized NGB showed that the disulfide bridge both defines the kinetics of NO dioxygenase activity and regulates appearance of the free ferrous deoxy-NGB, which is the redox active form of the protein in contrast to oxy-NGB. Our studies further identified a role for the distal histidine, interacting with the hexacoordinated iron atom of the heme, in oxidation kinetics. These findings may be relevant *in vivo*, for example in blocking apoptosis by reduction of ferric cytochrome *c*, and gentle tuning of NO concentration in the tissues.

---

Neuroglobin (Ngb) is the vertebrate globin that has been hypothesized to be involved in e.g. O<sub>2</sub> binding/supply, the metabolism of reactive nitrogen and oxygen species, apoptosis through different pathways, intracellular signaling, and cell protection during hypoxia and ischemia (1-6). Besides the central and peripheral nervous system and retina, Ngb is also expressed in endocrine tissues, hematopoietic stem cells, the gastrointestinal tract, and cancer cells (7,8). Although the first publication on the subject was in 2000, the *in vivo* role of Ngb is still uncertain. Studies on Ngb knock-out mice and regional gene expression did not clarify it further (3,9-13), but most of the reports in the topic supported its neuroprotective function at least under conditions of neuroglobin overexpression (11,14,15). Some histological data additionally indicated that Ngb can be involved in regulation of the circadian rhythm (sleep-wake cycle) (12,16) and protection of neurons from neurodegenerative disorders, such as Alzheimer's disease (17-19). Obviously, further *in vivo* and *in vitro* studies of Ngb are necessary to clarify its molecular mechanisms of action.

As other globins, e.g. myoglobin and hemoglobin, Ngb displays the three-over-three  $\alpha$ -helical sandwich structure. However, Ngb structurally differs somewhat from myoglobin and hemoglobin, suggesting a different

functional destination for Ngb compared to the classic globins (20). Both its weak O<sub>2</sub> binding affinity under physiological conditions (21) and its hexacoordinated structure of the iron atom of the heme leading to a possible intrinsic binding competition with external gaseous ligands such as O<sub>2</sub>, CO and NO, support the hypothesis that Ngb is not constructed to transport or store O<sub>2</sub> (22). Unclear mechanism of action encourages researchers for detailed studies of Ngb structure and properties.

The well-defined spectral properties of the heme in globins provide opportunities for studies by UV/Vis and EPR (20,23-25). Previously, myoglobin and hemoglobin have been extensively studied using electrochemical methods (26-30). However, electrochemistry has not yet been explored in studies of Ngb. Compared with other techniques, the electrochemical approach affords reduction or oxidation of Ngb by applying a potential to a working electrode without introduction of supplementary redox reagents.

Previously, two attempts were made to link NGB to electrode surfaces using modified gold and nanoporous indium tin oxide electrodes (31,32). Although electric communication of NGB with the electrodes was confirmed through spectral changes in the immobilized protein, voltammetry measurements were impossible because of low protein surface coverages and slow electron transfer kinetics. Recently we designed an efficient protocol for immobilization and electrochemical measurements of small hydrophilic proteins including NGB (33). It created the opportunity for kinetic studies of NGB using voltammetry techniques.

Due to reactivity of the heme iron, NGB can act through multiple molecular mechanisms which seem to be closely related to the redox and ligation states of the iron (21,34-50) (Fig. 1). Globins can express NO dioxygenase activity (oxidation of NO to nitrate in the presence of O<sub>2</sub> as shown in Fig. 1, reaction **d**). However, the relatively rapid autoxidation of Ngb (Fig. 1, reaction **c**) compels the introduction of a reductant or enzymatic reducing system to recover the ferrous form (Fig. 1, reaction **i**), which may interfere with measurements. Moreover, UV/Vis assays need a 5–10 μM concentration

of globins and an excess of NO, which exceeds by approximately two orders of magnitude the NO concentration *in vivo* (51). The advantage of the electrochemical approach is that Ngb can be rapidly converted from the ferric (Fe<sup>3+</sup>) to the ferrous (Fe<sup>2+</sup>) form at a polarized electrode, which facilitates control of the redox state of the protein and monitoring following chemical reactions in the presence of possible substrates such as O<sub>2</sub> and NO. Moreover, when the protein is immobilized in a thin layer at the electrode surface, a very low equilibrium concentrations of substrates can be introduced into the measuring cell without concern of its possible change because of reaction with the protein.

## RESULTS

*Electrochemical behavior of NGB* — The internal disulfide bridge between Cys46 and Cys55 in NGB defines oxygen-binding properties through the affinity of the distal histidine His64 (Fig. 1). The thiol/disulfide couple in NGB has a reduction potential of –0.194 V measured through equilibrium redox titration with glutathione (40). This value suggests that in a cell at normal conditions the disulfide bond is rather reduced (40), while the cysteine residues in the isolated protein are oxidized in air forming the disulfide bridge (21,34).

The NGB with the disulfide bridge will be referred to as NGB<sub>SS</sub>. To ease the study of NGB with the reduced disulfide bridge *in vitro*, a model protein with mutated surface cysteines (NGB\*) was created (21,52). NGB\* behaves in a similar way to NGB with the reduced disulfide bond, but it allows to work without precautions against oxidation of the thiols into the disulfide bridge (21). In this work we compared the behavior of NGB<sub>SS</sub> and NGB\* to assess the effect of the disulfide bridge on the properties and mechanisms of action of NGB.

Under N<sub>2</sub> atmosphere, NGB\* showed highly reversible electrochemical behavior when either dissolved in solution or immobilized on the electrodes (Fig. 2). The redox process at a formal potential  $E^{\circ'}$  of  $-0.136 \pm 0.005$  V corresponds to Fe<sup>3+/2+</sup> transition in the heme unit of NGB\*. Owing to hexacoordination of the iron, the heme unit undergoes little structural reorganization

during the reduction/oxidation transition, enhancing electron transfer kinetics (50,53). NGB<sub>SS</sub> behaved similarly with a formal potential  $E^{\circ'}$  of  $-0.126 \pm 0.006$  V, which we reported recently (33). A similar value was obtained by means of redox titration ( $-0.118 \pm 0.004$  V) (54). A slightly higher reduction potential of  $-0.103$  V was assessed by spectroelectrochemical measurements of the protein adsorbed at a transparent nanoporous indium tin oxide electrode (32).

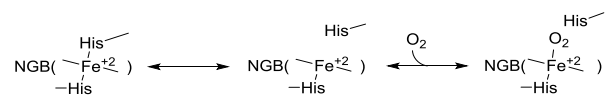
In equilibrium conditions, the protein will be reduced at potentials of the working electrode ( $E$ ) lower than the formal potential ( $E^{\circ'}$ ) and oxidized at higher ones according to the Nernst equation:

$$E = E^{\circ'} + 0.058 \cdot \lg([\text{Ox}]/[\text{Red}]),$$

where [Ox] and [Red] are the equilibrium concentrations of the oxidized and reduced forms.

It has been reported that NGB binds reversibly to O<sub>2</sub> (Fig. 1, reaction a) with a half-saturation pressure ( $P_{50}$ ) of 1–8 mm Hg depending on pH, temperature and the state of the internal disulfide bond (21). When the measuring buffer was saturated with air, the peak current of the heme unit in NGB\* was suppressed (Fig. 2C and D) due to formation of the oxy-form of NGB\*. The loss of the redox activity is related to the formation of the charge-transfer state involving orbitals of Fe<sup>2+</sup> and O<sub>2</sub> (55), which precludes the transition from Fe<sup>2+</sup> to Fe<sup>3+</sup> in the presence of O<sub>2</sub>.

*Effect of O<sub>2</sub> concentration* — The process of O<sub>2</sub> binding in NGB is preceded by a relatively slow distal histidine dissociation ( $k = 7$  s<sup>-1</sup> for NGB\* and 0.6 s<sup>-1</sup> for NGB<sub>SS</sub> as measured by flash photolysis (34)) as represented in following scheme:



The slow O<sub>2</sub> association/dissociation kinetics allowed us to perform voltammetry measurements of the ferrous deoxy-NGB without a noticeable shift in the equilibrium between oxy and deoxy forms during the measurements. The constant position of the peak potential at different levels of O<sub>2</sub> suggests that the kinetics of O<sub>2</sub>

dissociation are relatively slow compared to the time scale of the performed electrochemical measurements (56). However, faster scan rates can be applied if necessary. Thus, the peak current must be proportional to the amount of deoxy-NGB and can be converted to the fraction of deoxy-NGB as  $I_p/I_{p,0}$  or to the fraction of oxy-NGB as  $(1 - I_p/I_{p,0})$ , where  $I_{p,0}$  is the peak current in the absence of O<sub>2</sub> and  $I_p$  is the peak current at a given level of O<sub>2</sub>.

Fig. 3 shows the effect of oxygen concentration on the peak current for both NGB\* and NGB<sub>SS</sub>, obtained by DPV method. The plot of the oxy-NGB fraction against O<sub>2</sub> concentration is shown in Fig. 3C. The  $P_{50}$  was determined from the curves as  $1.4 \pm 0.5$  Torr for NGB<sub>SS</sub> and  $6.1 \pm 1.3$  Torr for NGB\*. Similar values were previously assessed in other studies (Table 1) based on flash photolysis and UV/Vis measurements (21,34).

*Effect of nitric oxide* — The effect of submicromolar NO concentration on NGB\* and NGB<sub>SS</sub> was studied in the presence of 30 Torr (50 μM) O<sub>2</sub>, which is close to the normal level of O<sub>2</sub> in the brain (57). Fig. 4A and B represents the corresponding data. When 50 μM O<sub>2</sub> was introduced into the measuring cell, the peak current of NGB\* was suppressed because of binding of NGB\* with O<sub>2</sub> as described in the previous section.

Introduction of NO into the cell restored the peak current proportional to the NO concentration (Fig. 4A and B). The increase in the peak current implies the increase of the steady-state concentration of the ferrous NGB\*, that was accumulated because of slow distal histidine dissociation during the oxygen-binding reaction becoming the rate-limiting step of the ongoing reaction (Fig. 5A). In the concentration range of 0.50–0.75 μM NO approximately 85% of NGB\* was accumulated in the ferrous form (Fig 4C). In these conditions the process was completely limited by O<sub>2</sub> binding and did not depend on NO concentration. At lower NO concentrations the amount of ferrous NGB was strictly proportional to the amount of NO.

It is noteworthy that NO concentrations higher than 1 μM resulted in a partial decrease in the ferrous NGB\* fraction, which can be explained by inhibition of the heme by

strongly bound NO (Fig. 1, reaction **b**). Fig. 4D shows the long-term effect of 1  $\mu\text{M}$  NO in the presence of 30  $\mu\text{M}$  O<sub>2</sub>. Because of the high affinity and stability of the NGB\*–NO complex (36), the level of ferrous NGB\* decreased by 60%. The initial level could not be restored by increasing O<sub>2</sub> concentration or N<sub>2</sub> purging, probably because of slow NO dissociation ( $k_{\text{off}} = 2 \cdot 10^{-4} \text{ s}^{-1}$ ) from the complex (36).

Surprisingly, NGB<sub>SS</sub> demonstrated only a minor increase of the ferrous NGB<sub>SS</sub> fraction with the NO concentration in the same conditions as NGB\* (Fig. 4C). The fraction of ferrous deoxy-NGB<sub>SS</sub> was 13% and 18% for 0.5  $\mu\text{M}$  and 1.0  $\mu\text{M}$  NO, respectively. As Fig. 5B illustrates, the disulfide bridge increased the rate of HisE7 dissociation and, apparently, shifted the rate-limiting step from O<sub>2</sub> binding to the NO-oxidation.

## DISCUSSION

A reductase that is capable of rapidly reducing NGB is not yet known. This problem limits assay studies because of autoxidation of NGB in the presence of O<sub>2</sub>. In this work we employed a polarized electrode as the reducing system which can recover the ferrous NGB from the oxidized ferric form. Such an approach allowed rapid reduction of the protein without introduction of any chemicals and simplified the study.

The technique for studying redox proteins on an electrode, also known as protein film voltammetry (58,59), was previously widely used for mechanistic studies of redox proteins. However, small hydrophilic proteins can easily desorb and dissolve in bulk. Thus, an appropriate immobilization technique must be used. Recently, we developed a gentle immobilization procedure based on a bis-silane cross-linker dissolved in water medium (33). Immobilized proteins including NGB could be retained at the surface without loss of redox activity or a noticeable shift of their redox potentials. Fast electron transfer kinetics allows us to reduce the protein rapidly and without diffusion limitation. Moreover, because of the small amount of the protein (approximately 0.04 pmol per electrode) and the large bulk volume, the consumption of O<sub>2</sub>

and NO from the bulk is negligible even when their concentrations are low. It permits reliable measurements for low concentration of NO and O<sub>2</sub>, while in assays using about 10  $\mu\text{M}$  protein concentration, studies in the presence of submicromolar NO would be impossible. Thus, the suggested approach allows (1) rapid electrochemical reduction of NGB and (2) equilibrium and kinetic measurements in low NO and O<sub>2</sub> concentration ranges.

It is known that the disulfide bridge regulates the affinity of NGB to bind oxygen (34). To study this effect a comparison was made between the wild type NGB (NGB<sub>SS</sub>) and NGB with mutated cysteines (NGB\*) (21,34). As ferrous NGB alone is electroactive but its complex with O<sub>2</sub> is not, we could titrate the protein by adding O<sub>2</sub> similar to the method used in UV/Vis assays but without introduction of any reduction agents. The obtained values of P<sub>50</sub> were  $6.1 \pm 1.3$  and  $1.4 \pm 0.5$  Torr for NGB\* and NGB<sub>SS</sub>, respectively, which is in good agreement with other reports (Table 1).

It should be mentioned that the published P<sub>50</sub> values demonstrate a noticeable distribution. Moreover, one may notice a difference in reports regarding the temperature dependence of O<sub>2</sub> affinity in NGB measured by equilibrium titration and flash photolysis (21,60). The results obtained in UV/Vis assays could depend on the rate of autoxidation of NGB and efficiency of the reducing system used at particular pH and temperature. The suggested electrochemical approach is free from these complications and can be further used for more detailed studies of the affinity of NGB to bind O<sub>2</sub> or other gases in different conditions.

Affinity to O<sub>2</sub> that is regulated through the disulfide bond is an intriguing feature of NGB but its role in O<sub>2</sub> supply/storage is unlikely for many reasons (3,4). The role of NGB as a possible NO dioxygenase is more supported since such a function is well-known for hemoglobin, myoglobin and especially for flavohemoglobin (61).

To the best of the authors' knowledge, only two works have been published with regard to an *in vitro* test of dioxygenase function in Ngb in the presence of O<sub>2</sub>,

conducted with mouse Ngb in air-saturated buffer (37) and with human NGB in the presence of 4% (30 Torr) O<sub>2</sub> (38). In both works the authors reported rapid NO oxidation by oxy-Ngb ( $k \approx 300 \text{ s}^{-1}$ ), which followed the rate-limiting distal histidine dissociation and O<sub>2</sub> binding ( $k \approx 0.4 \text{ s}^{-1}$ ) (37). The measurements with mouse Ngb were performed with 10 and 250  $\mu\text{M}$  NO, and the total kinetics were independent of NO concentration (37). The measurements with NGB by Smagghe et al. were conducted in the presence of 40  $\mu\text{M}$  NO (38). The ability to catalytically scavenge NO was directly related to the recovery rate of the ferrous form by the reduction system used. No data regarding physiologically relevant NO concentrations or an effect of the disulfide bond have yet been reported.

In contrast to the previous works (37,38), we were able to do measurements in a low NO concentration range and overcome the limitation of the slow re-reduction of NGB from its ferric form.

As a result, we found that O<sub>2</sub> binding kinetics in NGB\* are comparable to an NO oxidation rate up to 0.5  $\mu\text{M}$  NO concentration, which resulted in a split of the NGB\* into deoxy- and oxy-NGB\* fractions proportional to NO concentration. When the NO concentration was 0.5  $\mu\text{M}$  or higher, the kinetics of the dioxygenase activity were fully limited by O<sub>2</sub> binding, and almost all NGB\* was accumulated in the free ferrous form. In the same conditions, NGB<sub>SS</sub> did not show a similar effect, most probably because of the faster formation of the oxy form owing to tenfold faster distal histidine dissociation (34).

In conclusion, we demonstrated a new approach to study NGB in the presence of O<sub>2</sub> and NO that overcomes the limitation related to autoxidation of the protein and allows to work with submicromolar concentrations of effectors. The approach can be potentially extended to other hexacoordinate globins.

If we postulate the existence of a rapid reducing system for NGB *in vivo* (which should exist because of noticeable autoxidation of the protein in the presence of O<sub>2</sub>), then not only affinity to bind O<sub>2</sub> but also the rate of NO

oxidation to NO<sub>3</sub><sup>-</sup> and accumulation of the ferrous NGB is defined by the state of the internal disulfide bridge and NO concentration.

When the bridge is reduced, NGB can exist in the ferrous form even at high O<sub>2</sub> concentrations when a near micromolar or submicromolar amount of NO is present. This could be meaningful *in vivo*. For example, reduction of ferric cytochrome *c*, which has been hypothesized as an anti-apoptotic mechanism of action for NGB (46,47), can be accomplished only by the ferrous deoxy-NGB. Moreover, the ligand binding induces structural transition in NGB that prevents formation of the stable complex with G $\alpha_i$  (41) and, probably, other apoptosis related proteins (Fig. 1, reaction **g**). In the conditions of severe hypoxia, NGB–O<sub>2</sub> adduct can dissociate to form ferrous NGB. However, it may probably lose ability to interact with the apoptosis related proteins due to binding of NO whose concentration is elevated under hypoxia conditions. Our data suggest that ferrous (Fe<sup>+2</sup>) NGB can appear at a certain ratio of NO/O<sub>2</sub> concentrations and thus, reduce the ferric cytochrome *c* or bind the proteins involved in apoptosis (41-45), thus, leading to protection against neuronal death.

Finally, it is worth noting that NO plays multiple roles in the nervous system and in the pathophysiology of several neurological disorders (62). It can be assumed that NGB gently regulates NO concentration or acts as a sensor of NO/O<sub>2</sub> ratio in cells, generating a redox active form of NGB from the redox inactive oxy-form which exists at normal O<sub>2</sub> and very low NO concentrations.

## EXPERIMENTAL PROCEDURES

**Materials** — Recombinant human Ngb (NGB) and the triple mutant with replaced cysteine residues (Cys46Gly, Cys55Ser and Cys120Ser; NGB\*) were expressed and purified as described previously (52). Briefly, the recombinant expression plasmid with the pET3a vector was transformed in the *E. coli* strain BL21(DE3)pLysS. The cells were grown overnight at 37°C in 6 mL L-Broth containing ampicillin and chloramphenicol. Then, the culture was transferred into 250 mL TB medium containing ampicillin,

chloramphenicol and  $\delta$ -aminolevulinic acid. After reaching  $A_{600} = 0.8$ , the expression was induced by isopropyl-1-thio-D-galactopyranoside and continued overnight. After the preparation of a crude protein extract, NGB was purified using DEAE Sepharose Fast Flow and Sephacryl S-200 High Resolution chromatography, dialyzed against 5 mM pH 8.5 Tris-HCl and concentrated.

Inorganic salts, NaOH, H<sub>2</sub>SO<sub>4</sub>, 1,2-bis(trimethoxysilyl)ethane were purchased from Sigma-Aldrich (Belgium). 6-Mercapto-1-hexanol (>98.0 %) was sourced from TCI Europe N.V. (Belgium).

*Preparation of electrodes* — The commercial gold disk electrodes, 1.6 mm diameter (BASi, West Lafayette, IN, USA) were polished first on nylon pads (Buehler, Lake Bluff, IL, USA) using diamond suspensions of 3, 1 and 0.25  $\mu\text{m}$  particle size (DP-Spray, Struers, Ballerup, Denmark) in a supplier recommended lubricant (DP-Lubricant, Struers, Ballerup, Denmark), and on soft pads (Buehler, Lake Bluff, IL, USA) using a water based  $\gamma$ -alumina slurry of 50 nm particle size (SPI Supplies, West Chester, PA, USA). The electrodes were sonicated in ethanol and ultrapure water after each polishing step. Next, the electrodes were electrochemically treated in 0.5 M NaOH and 0.5 M H<sub>2</sub>SO<sub>4</sub> until a repetitive voltammogram of polycrystalline gold was achieved (63,64). Finally, the electrodes were left in 8 mM 6-mercapto-1-hexanol solution in ultrapure water for approximately 20 h.

Afterwards, 1.8  $\mu\text{L}$  of a mixture consisting of 15  $\mu\text{M}$  protein and 10 mM 1,2-bis(trimethoxysilyl)ethane in 50 mM pH 7 KH<sub>2</sub>PO<sub>4</sub> buffer was placed on the electrodes and dried at room temperature for 1 h. The obtained surface coverage of the surface-confined NGB was approximately 2 pmol/cm<sup>2</sup>.

Cyclic (CV) and differential pulse voltammetry (DPV) were conducted in pH 7.4 PBS buffer using a conventional three-electrode cell and  $\mu$ Autolab III electrochemical interface (Metrohm-Autolab BV, the Netherlands). A saturated calomel electrode (Radiometer, Denmark; +0.244 V vs standard hydrogen electrode at 25°C) and a glassy carbon rod were used as reference and counter

electrode, respectively. All potentials are given versus the standard hydrogen electrode (SHE).

Background CV behavior of MH modified electrodes was carefully checked to ensure the quality of the electrode preparation and stability of the electrodes. Contaminated electrodes and electrodes with a defective MH layer (which could be disclosed due to an increased background current under N<sub>2</sub> atmosphere) demonstrated inappropriate long-term stability and were discarded.

*O<sub>2</sub> binding* — The measuring buffer (30 mL) was purged with N<sub>2</sub> for 1 h in advance and for at least 20 min after the protein electrodes were inserted into the thermostatic (25.0  $\pm$  0.2 °C) electrochemical cell. CV and DPV performances of the electrodes were recorded to ensure good stability and appropriate immobilization of NGB. Next, DPV curves were sequentially recorded starting from -0.3 V till +0.05 V with a conditioning step of 1 min before each measurement, when the potential was set again to -0.3 V to keep the protein in the reduced form. After recording at least five consecutive DPV curves under N<sub>2</sub> to ensure stable peak intensity, a certain volume of the air-saturated buffer, equilibrated at the same temperature, was injected using an air-tight syringe. For each concentration the measurements were repeated at least twice to ensure the stable value of the peak current after introduction of O<sub>2</sub>.

*NO metabolism* — A saturated water solution of NO was prepared as previously described (65,66). Briefly, 2 M H<sub>2</sub>SO<sub>4</sub> was carefully added drop-wise into saturated NaNO<sub>2</sub> preliminarily purged with nitrogen. The disproportional reaction resulted in the formation of NO which was directed to pass through a washing bottle containing 30% NaOH and two vials with ultrapure water. The solution from the second vial was used in the experiments. Under room temperature (22 °C) and normal pressure conditions, the saturated concentration of NO in water is close to 2.0 mM (67). Saturated NO solution was added to the electrochemical cell using an air-tight Hamilton syringe to get NO concentrations in the range from 0.05 to 1.25  $\mu\text{M}$ . The measurements were done in the presence of 50  $\mu\text{M}$  (30 Torr) O<sub>2</sub> at 25°C.

**ACKNOWLEDGEMENT**

This work was supported by the Fund for Scientific Research – Flanders (FWO) (Grant G.0687.13) and the GOA-BOF UA 2013–2016 (project-ID 28312).

**CONFLICT OF INTEREST**

The authors declare that they have no conflicts of interest with the contents of this article.

**AUTHOR CONTRIBUTIONS**

KDW and ST designed research and analyzed all data; ST conducted most of the experiments and wrote most of the paper; MdJ conducted preliminary experiments on the immobilization and electrochemical characterization of NGB; EL purified and characterized samples of NGB and NGB\*, SD contributed to interpretation of data and revised the paper.

**REFERENCES**

1. Burmester, T., Weich, B., Reinhardt, S., and Hankeln, T. (2000) A vertebrate globin expressed in the brain. *Nature* **407**, 520
2. Tejero, J., and Gladwin, M. T. (2014) The globin superfamily: functions in nitric oxide formation and decay. *Biol. Chem.* **395**, 631
3. Burmester, T., and Hankeln, T. (2014) Function and evolution of vertebrate globins. *Acta Physiol.* **211**, 501
4. Ascenzi, P., Gustincich, S., and Marino, M. (2014) Mammalian nerve globins in search of functions. *IUBMB life* **66**, 268
5. Haines, B., Demaria, M., Mao, X., Xie, L., Campisi, J., Jin, K., and Greenberg, D. A. (2012) Hypoxia-inducible factor-1 and neuroglobin expression. *Neurosci. Lett.* **514**, 137
6. Jin, K., Mao, X. O., Xie, L., Khan, A. A., and Greenberg, D. A. (2008) Neuroglobin protects against nitric oxide toxicity. *Neurosci. Lett.* **430**, 135
7. Emara, M., Turner, A. R., and Allalunis-Turner, J. (2010) Hypoxic regulation of cytoglobin and neuroglobin expression in human normal and tumor tissues. *Cancer Cell Int.* **10**, 33
8. Fiocchetti, M., Nuzzo, M. T., Totta, P., Acconcia, F., Ascenzi, P., and Marino, M. (2014) Neuroglobin, a pro-survival player in estrogen receptor alpha-positive cancer cells. *Cell Death Dis.* **5**, 10
9. Fordel, E., Thijs, L., Moens, L., and Dewilde, S. (2007) Neuroglobin and cytoglobin expression in mice - Evidence for a correlation with reactive oxygen species scavenging. *FEBS J.* **274**, 1312
10. Hundahl, C. A., Luuk, H., Ilmarj, S., Falktoft, B., Raida, Z., Vikesaa, J., Friis-Hansen, L., and Hay-Schmidt, A. (2011) Neuroglobin-deficiency exacerbates Hif1A and c-FOS response, but does not affect neuronal survival during severe hypoxia in vivo. *PLoS One* **6**, e28160
11. Raida, Z., Hundahl, C. A., Kelsen, J., Nyengaard, J. R., and Hay-Schmidt, A. (2012) Reduced infarct size in neuroglobin-null mice after experimental stroke in vivo. *Exp. Transl. Stroke Med.* **4**, 15
12. Hundahl, C. A., Allen, G. C., Hannibal, J., Kjaer, K., Rehfeld, J. F., Dewilde, S., Nyengaard, J. R., Kelsen, J., and Hay-Schmidt, A. (2010) Anatomical characterization of cytoglobin and neuroglobin mRNA and protein expression in the mouse brain. *Brain Res.* **1331**, 58
13. Schmidt-Kastner, R., Haberkamp, M., Schmitz, C., Hankeln, T., and Burmester, T. (2006) Neuroglobin mRNA expression after transient global brain ischemia and prolonged hypoxia in cell culture. *Brain Res.* **1103**, 173



14. Fiocchetti, M., De Marinis, E., Ascenzi, P., and Marino, M. (2013) Neuroglobin and neuronal cell survival. *Biochim. Biophys. Acta, Proteins Proteomics* **1834**, 1744
15. Raida, Z., Hundahl, C. A., Nyengaard, J. R., and Hay-Schmidt, A. (2013) Neuroglobin over expressing mice: expression pattern and effect on brain ischemic infarct size. *PLoS One* **8**, e76565
16. Hundahl, C. A., Fahrenkrug, J., Hay-Schmidt, A., Georg, B., Faltoft, B., and Hannibal, J. (2012) Circadian behaviour in neuroglobin deficient mice. *PLoS One* **7**, e34462
17. Khan, A. A., Mao, X. O., Banwait, S., Jin, K., and Greenberg, D. A. (2007) Neuroglobin attenuates beta-amyloid neurotoxicity in vitro and transgenic Alzheimer phenotype in vivo. *Proc. Natl. Acad. Sci. U. S. A.* **104**, 19114
18. Chen, L.-M., Xiong, Y.-S., Kong, F.-L., Qu, M., Wang, Q., Chen, X.-Q., Wang, J.-Z., and Zhu, L.-Q. (2012) Neuroglobin attenuates Alzheimer-like tau hyperphosphorylation by activating Akt signaling. *J. Neurochem.* **120**, 157
19. Ferrer, I., Gomez, A., Carmona, M., Huesa, G., Porta, S., Riera-Codina, M., Biagioli, M., Gustincich, S., and Aso, E. (2011) Neuronal Hemoglobin is Reduced in Alzheimer's Disease, Argyrophilic Grain Disease, Parkinson's Disease, and Dementia with Lewy Bodies. *J. Alzheimer's Dis.* **23**, 537
20. Dewilde, S., Kiger, L., Burmester, T., Hankeln, T., Baudin-Creuz, V., Aerts, T., Marden, M. C., Caubergs, R., and Moens, L. (2001) Biochemical characterization and ligand binding properties of neuroglobin, a novel member of the globin family. *J. Biol. Chem.* **276**, 38949
21. Fago, A., Hundahl, C., Dewilde, S., Gilany, K., Moens, L., and Weber, R. E. (2004) Allosteric regulation and temperature dependence of oxygen binding in human neuroglobin and cytoglobin. Molecular mechanisms and physiological significance. *J. Biol. Chem.* **279**, 44417
22. Hankeln, T., Ebner, B., Fuchs, C., Gerlach, F., Haberkamp, M., Laufs, T. L., Roesner, A., Schmidt, M., Weich, B., Wystub, S., Saaler-Reinhardt, S., Reuss, S., Bolognesi, M., De Sanctis, D., Marden, M. C., Kiger, L., Moens, L., Dewilde, S., Nevo, E., Avivi, A., Weber, R. E., Fago, A., and Burmester, T. (2005) Neuroglobin and cytoglobin in search of their role in the vertebrate globin family. *J. Inorg. Biochem.* **99**, 110
23. Van Doorslaer, S., Trandafir, F., Harmer, J. R., Moens, L., and Dewilde, S. (2014) EPR analysis of cyanide complexes of wild-type human neuroglobin and mutants in comparison to horse heart myoglobin. *Biophys. Chem.* **190**, 8
24. Walker, F. A. (2006) The heme environment of mouse neuroglobin: histidine imidazole plane orientations obtained from solution NMR and EPR spectroscopy as compared with X-ray crystallography. *J. Biol. Inorg. Chem.* **11**, 391
25. Vinck, E., Van Doorslaer, S., Dewilde, S., Mitrikas, G., Schweiger, A., and Moens, L. (2006) Analyzing heme proteins using EPR techniques: the heme-pocket structure of ferric mouse neuroglobin. *J. Biol. Inorg. Chem.* **11**, 467
26. Fan, C. H., Chen, X. C., Li, G. X., Zhu, J. Q., Zhu, D. X., and Scheer, H. (2000) Direct electrochemical characterization of the interaction between haemoglobin and nitric oxide. *Phys. Chem. Chem. Phys.* **2**, 4409
27. Scheller, F. W., Bistolos, N., Liu, S., Janchen, M., Katterle, M., and Wollenberger, U. (2005) Thirty years of haemoglobin electrochemistry. *Adv. Colloid Interface Sci.* **116**, 111

28. Kroning, S., Scheller, F. W., Wollenberger, U., and Lisdat, F. (2004) Myoglobin-clay electrode for nitric oxide (NO) detection in solution. *Electroanalysis* **16**, 253
29. Taniguchi, I., Watanabe, K., Tominaga, M., and Hawkridge, F. M. (1992) Direct electron-transfer of horse heart myoglobin at an indium oxide electrode. *J. Electroanal. Chem.* **333**, 331
30. King, B. C., Hawkridge, F. M., and Hoffman, B. M. (1992) Electrochemical studies of cyanometmyoglobin and metmyoglobin - implications for long-range electron-transfer in proteins. *J. Am. Chem. Soc.* **114**, 10603
31. Balland, V., Lecomte, S., and Limoges, B. (2009) Characterization of the electron transfer of a ferrocene redox probe and a histidine-tagged hemoprotein specifically bound to a nitrilotriacetic-terminated self-assembled monolayer. *Langmuir* **25**, 6532
32. Schaming, D., Renault, C., Tucker, R. T., Lau-Truong, S., Aubard, J., Brett, M. J., Balland, V., and Limoges, B. (2012) Spectroelectrochemical characterization of small hemoproteins adsorbed within nanostructured mesoporous ITO electrodes. *Langmuir* **28**, 14065
33. Trashin, S., de Jong, M., Meynen, V., Dewilde, S., and De Wael, K. (2016) Attaching redox proteins onto electrode surfaces by bis-silane. *ChemElectroChem*, Article first published online: 21 April 2016, DOI: 2010.1002/celec.201600021
34. Hamdane, D., Kiger, L., Dewilde, S., Green, B. N., Pesce, A., Uzan, J., Burmester, T., Hankeln, T., Bolognesi, M., Moens, L., and Marden, M. C. (2003) The redox state of the cell regulates the ligand binding affinity of human neuroglobin and cytoglobin. *J. Biol. Chem.* **278**, 51713
35. Kiger, L., Uzan, J., Dewilde, S., Burmester, T., Hankeln, T., Moens, L., Hamdane, D., Baudin-Creuzza, V., and Marden, M. (2004) Neuroglobin ligand binding kinetics. *IUBMB life* **56**, 709
36. Van Doorslaer, S., Dewilde, S., Kiger, L., Nistor, S. V., Goovaerts, E., Marden, M. C., and Moens, L. (2003) Nitric oxide binding properties of neuroglobin. A characterization by EPR and flash photolysis. *J. Biol. Chem.* **278**, 4919
37. Brunori, M., Giuffre, A., Nienhaus, K., Nienhaus, G. U., Scandurra, F. M., and Vallone, B. (2005) Neuroglobin, nitric oxide, and oxygen: functional pathways and conformational changes. *Proc. Natl. Acad. Sci. U. S. A.* **102**, 8483
38. Smagghe, B. J., Trent III, J. T., and Hargrove, M. S. (2008) NO dioxygenase activity in hemoglobins is ubiquitous in vitro, but limited by reduction in vivo. *PLoS One* **3**, e2039
39. Herold, S., Fago, A., Weber, R. E., Dewilde, S., and Moens, L. (2004) Reactivity studies of the Fe(III) and Fe(II)NO forms of human neuroglobin reveal a potential role against oxidative stress. *J. Biol. Chem.* **279**, 22841
40. Tiso, M., Tejero, J., Basu, S., Azarov, I., Wang, X., Simplaceanu, V., Frizzell, S., Jayaraman, T., Geary, L., Shapiro, C., Ho, C., Shiva, S., Kim-Shapiro, D. B., and Gladwin, M. T. (2011) Human Neuroglobin Functions as a Redox-regulated Nitrite Reductase. *J. Biol. Chem.* **286**, 18277
41. Wakasugi, K., Nakano, T., and Morishima, I. (2003) Oxidized human neuroglobin acts as a heterotrimeric G $\alpha$  protein guanine nucleotide dissociation inhibitor. *J. Biol. Chem.* **278**, 36505
42. Yu, Z., Liu, N., Li, Y., Xu, J., and Wang, X. (2013) Neuroglobin overexpression inhibits oxygen-glucose deprivation-induced mitochondrial permeability transition pore opening in primary cultured mouse cortical neurons. *Neurobiol. Dis.* **56**, 95

43. Wakasugi, K., Nakano, T., Kitatsuji, C., and Morishima, I. (2004) Human neuroglobin interacts with flotillin-1, a lipid raft microdomain-associated protein. *Biochem. Biophys. Res. Commun.* **318**, 453
44. Khan, A. A., Mao, X. O., Banwait, S., DerMardirossian, C. M., Bokoch, G. M., Jin, K., and Greenberg, D. A. (2008) Regulation of hypoxic neuronal death signaling by neuroglobin. *FASEB J.* **22**, 1737
45. Yu, Z., Zhang, Y., Liu, N., Yuan, J., Lin, L., Zhuge, Q., Xiao, J., and Wang, X. (2015) Roles of Neuroglobin Binding to Mitochondrial Complex III Subunit Cytochrome *c*1 in Oxygen-Glucose Deprivation-Induced Neurotoxicity in Primary Neurons. *Mol. Neurobiol.*, 1
46. Fago, A., Mathews, A. J., Moens, L., Dewilde, S., and Brittain, T. (2006) The reaction of neuroglobin with potential redox protein partners cytochrome *b*<sub>5</sub> and cytochrome *c*. *FEBS Lett.* **580**, 4884
47. Raychaudhuri, S., Skommer, J., Henty, K., Birch, N., and Brittain, T. (2010) Neuroglobin protects nerve cells from apoptosis by inhibiting the intrinsic pathway of cell death. *Apoptosis* **15**, 401
48. Bønding, S. H., Henty, K., Dingley, A. J., and Brittain, T. (2008) The binding of cytochrome *c* to neuroglobin: a docking and surface plasmon resonance study. *Int. J. Biol. Macromol.* **43**, 295
49. Tiwari, P. B., Astudillo, L., Pham, K., Wang, X. W., He, J., Bemad, S., Derrien, V., Sebban, P., Miksovska, J., and Darici, Y. (2015) Characterization of molecular mechanism of neuroglobin binding to cytochrome *c*: A surface plasmon resonance and isothermal titration calorimetry study. *Inorg. Chem. Commun.* **62**, 37
50. Weiland, T. R., Kundu, S., Trent, J. T., 3rd, Hoy, J. A., and Hargrove, M. S. (2004) Bis-histidyl hexacoordination in hemoglobins facilitates heme reduction kinetics. *J. Am. Chem. Soc.* **126**, 11930
51. Hall, C. N., and Garthwaite, J. (2009) What is the real physiological NO concentration in vivo? *Nitric Oxide* **21**, 92
52. Dewilde, S., Mees, K., Kiger, L., Lechauve, C., Marden, M. C., Pesce, A., Bolognesi, M., and Moens, L. (2008) Expression, purification, and crystallization of neuro- and cytoglobin. *Methods Enzymol.* **436**, 341
53. Kiger, L., Tilleman, L., Geuens, E., Hoogewijs, D., Lechauve, C., Moens, L., Dewilde, S., and Marden, M. C. (2011) Electron transfer function versus oxygen delivery: a comparative study for several hexacoordinated globins across the animal kingdom. *PLoS One* **6**, e20478
54. Tejero, J., Sparacino-Watkins, C. E., Ragireddy, V., Frizzell, S., and Gladwin, M. T. (2015) Exploring the mechanisms of the reductase activity of neuroglobin by site-directed mutagenesis of the heme distal pocket. *Biochemistry* **54**, 722
55. Chen, H., Ikeda-Saito, M., and Shaik, S. (2008) Nature of the Fe-O<sub>2</sub> bonding in oxy-myoglobin: effect of the protein. *J. Am. Chem. Soc.* **130**, 14778
56. Gulaboski, R., Mirčeski, V., Lovrić, M., and Bogeski, I. (2005) Theoretical study of a surface electrode reaction preceded by a homogeneous chemical reaction under conditions of square-wave voltammetry. *Electrochem. Commun.* **7**, 515
57. Carreau, A., El Hafny-Rahbi, B., Matejuk, A., Grillon, C., and Kieda, C. (2011) Why is the partial oxygen pressure of human tissues a crucial parameter? Small molecules and hypoxia. *J. Cell. Mol. Med.* **15**, 1239

58. Armstrong, F. A., Heering, H. A., and Hirst, J. (1997) Reaction of complex metalloproteins studied by protein-film voltammetry. *Chem. Soc. Rev.* **26**, 169
59. Gulaboski, R., Mirčeski, V., Bogeski, I., and Hoth, M. (2011) Protein film voltammetry: electrochemical enzymatic spectroscopy. A review on recent progress. *J. Solid State Electrochem.* **16**, 2315
60. Uzan, J., Dewilde, S., Burmester, T., Hankeln, T., Moens, L., Hamdane, D., Marden, M. C., and Kiger, L. (2004) Neuroglobin and other hexacoordinated hemoglobins show a weak temperature dependence of oxygen binding. *Biophys. J.* **87**, 1196
61. Gardner, P. R. (2005) Nitric oxide dioxygenase function and mechanism of flavohemoglobin, hemoglobin, myoglobin and their associated reductases. *J. Inorg. Biochem.* **99**, 247
62. Jain, K. K. (2013) Role of Nitric Oxide in Neurological Disorders. in *Applications of Biotechnology in Neurology* (Jain, K. K. ed.), Humana Press, New York. pp 249-282
63. Juodkazis, K., Juodkazyt, J., Šebeka, B., and Lukinskas, A. (1999) Cyclic voltammetric studies on the reduction of a gold oxide surface layer. *Electrochem. Commun.* **1**, 315
64. Piela, B., and Wrona, P. K. (1995) Capacitance of the gold electrode in 0.5 M H<sub>2</sub>SO<sub>4</sub> solution: a.c. impedance studies. *J. Electroanal. Chem.* **388**, 69
65. Wang, Y., and Hu, S. (2006) A novel nitric oxide biosensor based on electropolymerization poly(toluidine blue) film electrode and its application to nitric oxide released in liver homogenate. *Biosens. Bioelectron.* **22**, 10
66. Lim, M. D., Lorkovic, I. M., and Ford, P. C. (2005) The preparation of anaerobic nitric oxide solutions for the study of heme model systems in aqueous and nonaqueous media: Some consequences of NO<sub>x</sub> impurities. in *Nitric Oxide: Part E* (Packer, L., and Cadenas, E. eds.), Elsevier Academic Press Inc, San Diego. pp 3-17
67. Young, C. L. (1981) *IUPAC solubility data series. Oxides of Nitrogen*, Pergamon Press, Oxford

## FOOTNOTES

The abbreviations used are: Ngb, neuroglobin; NGB, human neuroglobin; NGB\*, NGB with mutated surface cysteines; NGB<sub>SS</sub>, NGB with the internal disulfide bridge; EPR, electron paramagnetic resonance; PBS, phosphate-buffered saline; CV, cyclic voltammetry; DPV, differential pulse voltammetry; UV/Vis, ultraviolet-visible spectrophotometry.

## FIGURE LEGENDS

**FIGURE 1.** The relation of the redox and ligation states of the heme iron and NGB reactivity. (a) Ferrous (Fe<sup>2+</sup>) NGB reacts with O<sub>2</sub> to form the O<sub>2</sub> adduct. The dissociation of the distal histidine limits the binding kinetics due a low dissociation rate constant of 0.6 s<sup>-1</sup> and 7 s<sup>-1</sup> for NGB with reduced and oxidized state of the internal disulfide bridge respectively (34,35). The P<sub>50</sub> value was reported in the range of 1-8 Torr depending on pH, temperature and the state of the internal disulfide bound (21). (b) Ferrous NGB reacts with NO leading to the nitrosyl ligated form with K<sub>d</sub> ≈ 1 nM and a slow dissociation rate constant k<sub>off</sub> ≈ 10<sup>-4</sup> – 10<sup>-3</sup> s<sup>-1</sup> (37). (c) NGB-O<sub>2</sub> adduct is prone to autoxidation with k ≈ 0.17 min<sup>-1</sup> (21). Similar to myoglobin and hemoglobin, NGB has been reported as a scavenger of reactive oxygen and nitrogen species (ROS, RNS): (d) NGB shows NO dioxygenase activity with k<sub>cat</sub> ≈ 300 s<sup>-1</sup> (37,38); (e) nitrosyl ferrous NGB but not ferric (Fe<sup>3+</sup>) NGB can scavenge peroxynitrite with k<sub>cat</sub> ≈ 1.3·10<sup>5</sup> M<sup>-1</sup> s<sup>-1</sup>

(39); **(f)** ferrous (Fe<sup>2+</sup>) NGB can reduce nitrite (NO<sub>2</sub><sup>-</sup>) although with a relatively low rate constant of 0.06 and 0.12 M<sup>-1</sup> s<sup>-1</sup> for NGB with the reduced and oxidized state of the disulfide bridge respectively (40). The role of NGB in blocking apoptosis through binding other proteins has been also suggested in the literature: **(g)** NGB can bind to the GDP-bound form of the  $\alpha$ -subunit of heterotrimeric G-protein (G $\alpha_i$ ) with K<sub>d</sub>  $\approx$  6·10<sup>2</sup> nM (41). Immunoprecipitation technique revealed binding of NGB to voltage-dependent anion channel (VDAC) (42), Flotillin-1 (43), two members of the Rho GTPase family (Rac1 and Rho A), as well as the Pak1 kinase (44), and a subunit of the mitochondrial complex III Cytochrome *c*1 (45). It has been found that the conformational transition in NGB upon binding ligands such as O<sub>2</sub> and NO can prevent NGB binding to G $\alpha_i$ . Similar mechanisms may regulate binding to other proteins. **(h)** Moreover, ferrous NGB is capable to reduce rapidly ferric Cytochrome *c* (Cyt *c*) with a kinetic constant of 2 · 10<sup>7</sup> M<sup>-1</sup>s<sup>-1</sup> (46), which seems to be facilitated by an appropriate docking between two proteins (47,48). Interaction between Cyt *c* and NGB goes through a rapid transient binding with a relatively high dissociation constant K<sub>d</sub>  $\approx$  120  $\mu$ M (48), which decreases in low ionic strength buffer suggesting that the interaction is largely electrostatic in nature (48,49). **(i)** The reaction that is responsible for one-electron reduction of the ferric (Fe<sup>3+</sup>) to ferrous (Fe<sup>2+</sup>) form is not known yet. It can be driven by an enzyme process or a low molecular weight redox compound/mediator. Noteworthy, hexacoordination of the heme iron favors reduction kinetics comparing to pentacoordinated analogues (50).

**FIGURE 2.** CV and DPV behavior of NGB\* in PBS buffer solution (A, B) and immobilized on the gold electrodes (C, D). Concentration of the dissolved NGB\*, 20  $\mu$ M; surface density of the immobilized NGB\*, 2 pmol/cm<sup>2</sup>; CV scan rate, 20 mV/s; DPV modulation amplitude, 20 mV; modulation time, 0.05 s; interval time, 0.5 s. The arrows denote scan directions. Blank voltammograms are shown by dashed lines (in green) and curves recorded in the air-saturated buffer are presented by dashed-dotted lines (in blue).

**FIGURE 3.** Behavior of NGB in the presence of different levels of O<sub>2</sub>. (A, B) Change in voltammograms with increase of O<sub>2</sub> level in the presence of NGB\* and NGB<sub>SS</sub>; (C) determined fraction of the oxygenated NGB in equilibrium with the ferrous (Fe<sup>2+</sup>) NGB as a function of O<sub>2</sub> concentration. Error bars show standard deviation for three consecutive measurements. PBS pH 7.4, 25°C.

**FIGURE 4.** Behavior of NGB in the presence of 30 Torr O<sub>2</sub> and submicromolar NO concentrations: (A) change in DPV curves for NGB\*; (B) the DPV curves after baseline correction; (C) dependence of the steady state deoxy-NGB fraction on NO concentration in the presence of 30 Torr O<sub>2</sub>. Average values of three separate titration curves are plotted, with the standard deviation values. (D) Stability of deoxy-NGB\* in the presence of 20 Torr O<sub>2</sub> and 1  $\mu$ M NO. Arrows denote direction of changes. PBS pH 7.4, 25°C.

**FIGURE 5.** The mechanism of NGB transitions in the presence of 0.5  $\mu$ M NO and 30 Torr O<sub>2</sub>: (a) behavior of NGB\* which models the protein with the opened disulfide bridge that favors the hexacoordinate ferrous form; (b) behavior of NGB<sub>SS</sub> which is the protein with the disulfide bridge that favors the oxygenated form. Broken arrows indicate a rate limiting step and the bold red structures depict an accumulated form.

**TABLE 1.** Comparison of P<sub>50</sub> values for NGB obtained by different methods

	Method	Conditions	P50 (Torr)	Reference
NGB*	Voltammetry	PBS, pH 7.4, 25°C	6.1 ± 1.3 <sup>[a]</sup>	This work
NGB <sub>SS</sub>	Voltammetry	PBS, pH 7.4, 25°C	1.4 ± 0.5 <sup>[a]</sup>	This work
NGB* <sup>[b]</sup>	Equilibrium UV/Vis <sup>[c]</sup>	Bis-Tris/Hepes, pH 7.0, 25°C	5	Fago et al. (40)
NGB* <sup>[b]</sup>	Equilibrium UV/Vis <sup>[c]</sup>	Bis-Tris/Hepes, pH 7.6, 20°C	2.6	Fago et al. (40)
NGB <sub>SS</sub>	Equilibrium UV/Vis <sup>[c]</sup>	Bis-Tris/Hepes, pH 7.6, 20°C	0.67	Fago et al. (40)
NGB*	Flash photolysis	Phosphate, pH 7.0, 25°C	10	Hamdane et al. (41)
NGB <sub>SS</sub>	Flash photolysis	Phosphate, pH 7.0, 25°C	0.9	Hamdane et al. (41)
NGB+DTT	Flash photolysis	Phosphate, pH 7.0, 25°C	8.4	Hamdane et al. (41)

<sup>[a]</sup>average ± standard error (n=4); <sup>[b]</sup>No difference between NGB\* and NGB+DTT was reported; <sup>[c]</sup>measured on an ultrathin layer of protein sample using a gas diffusion chamber.

Figure 1.

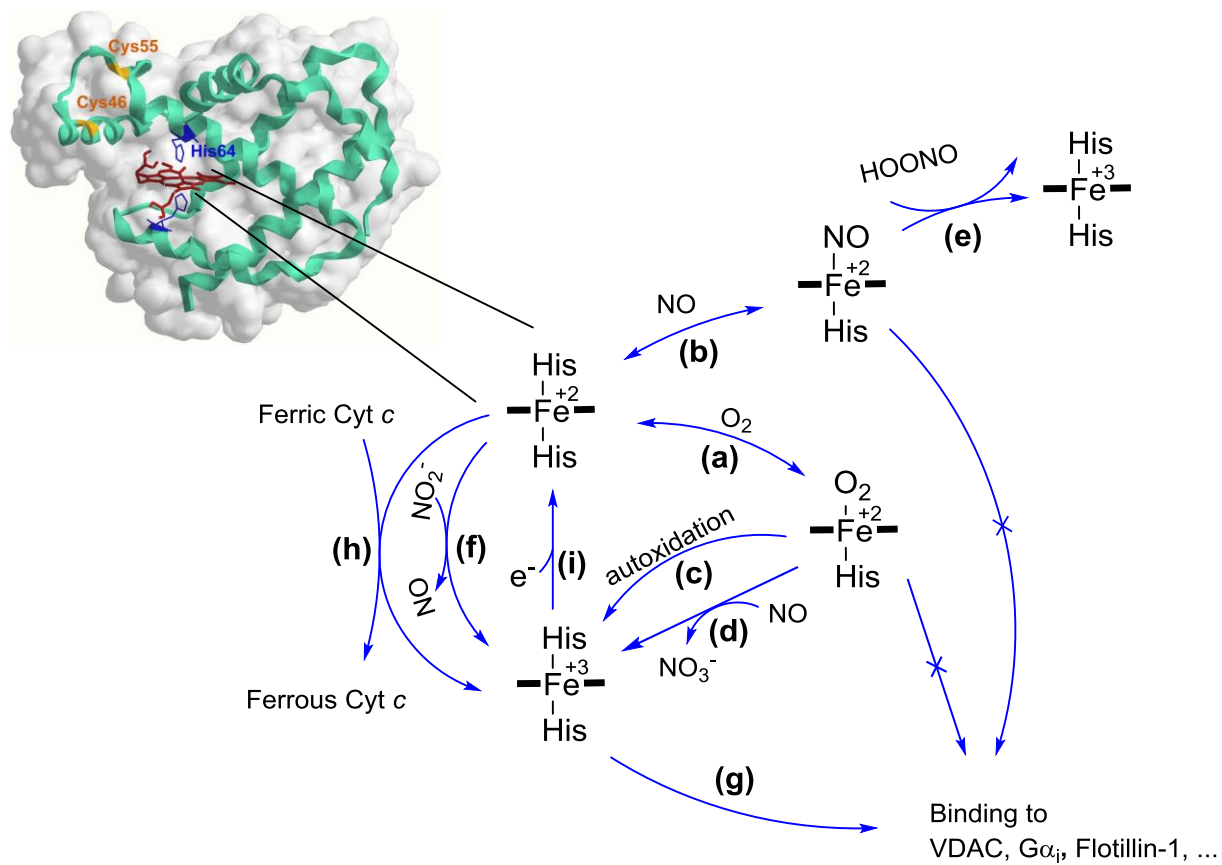


**Figure 2.**

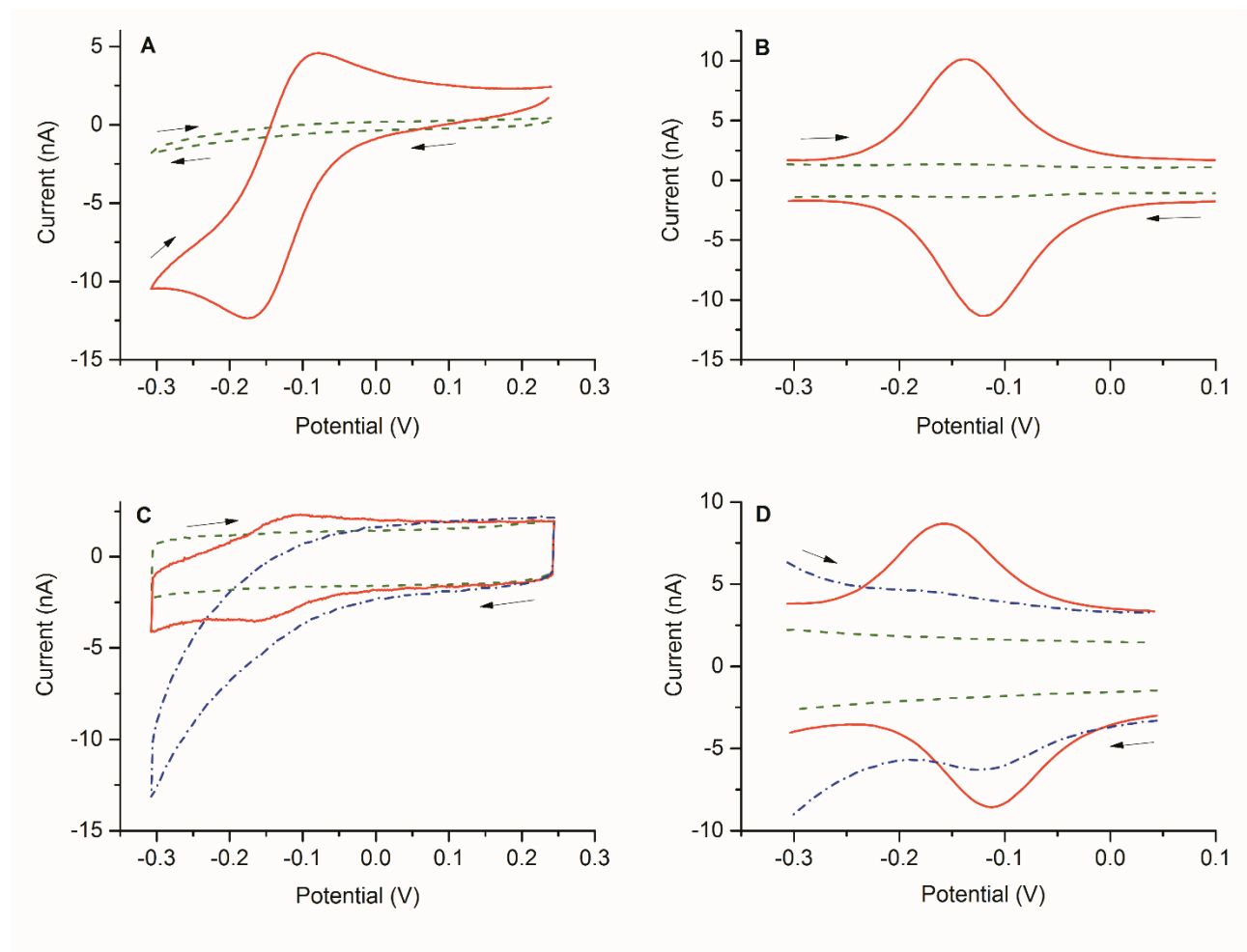




**Figure 3.**

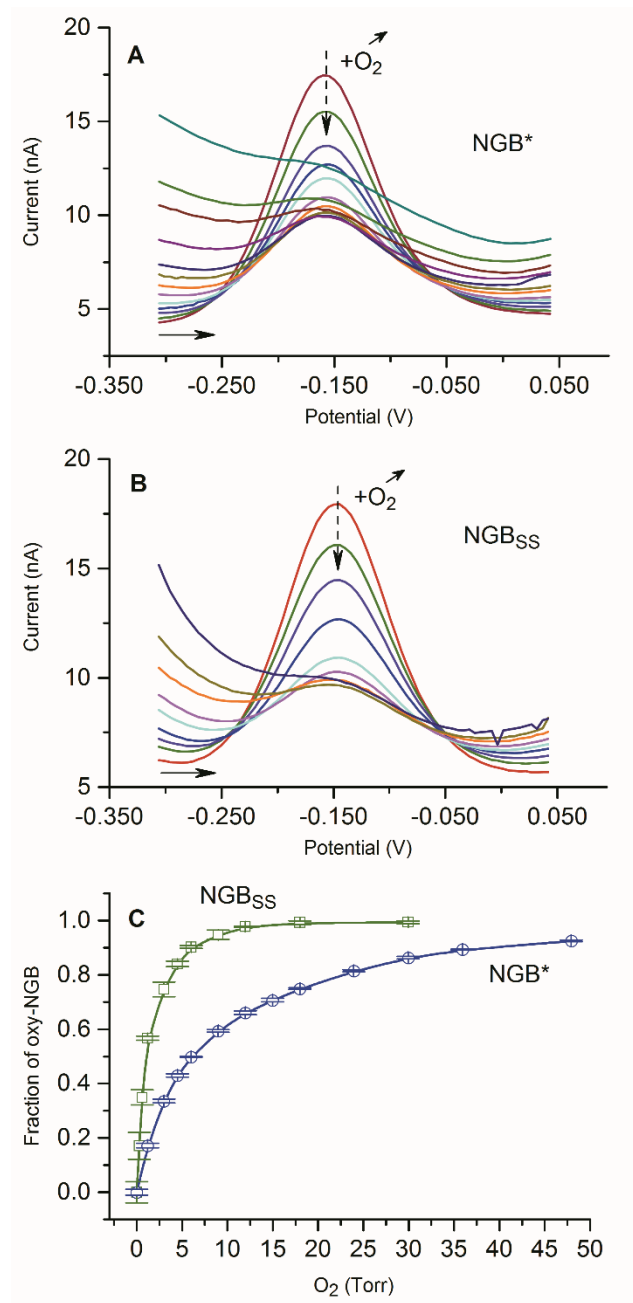


Figure 4.

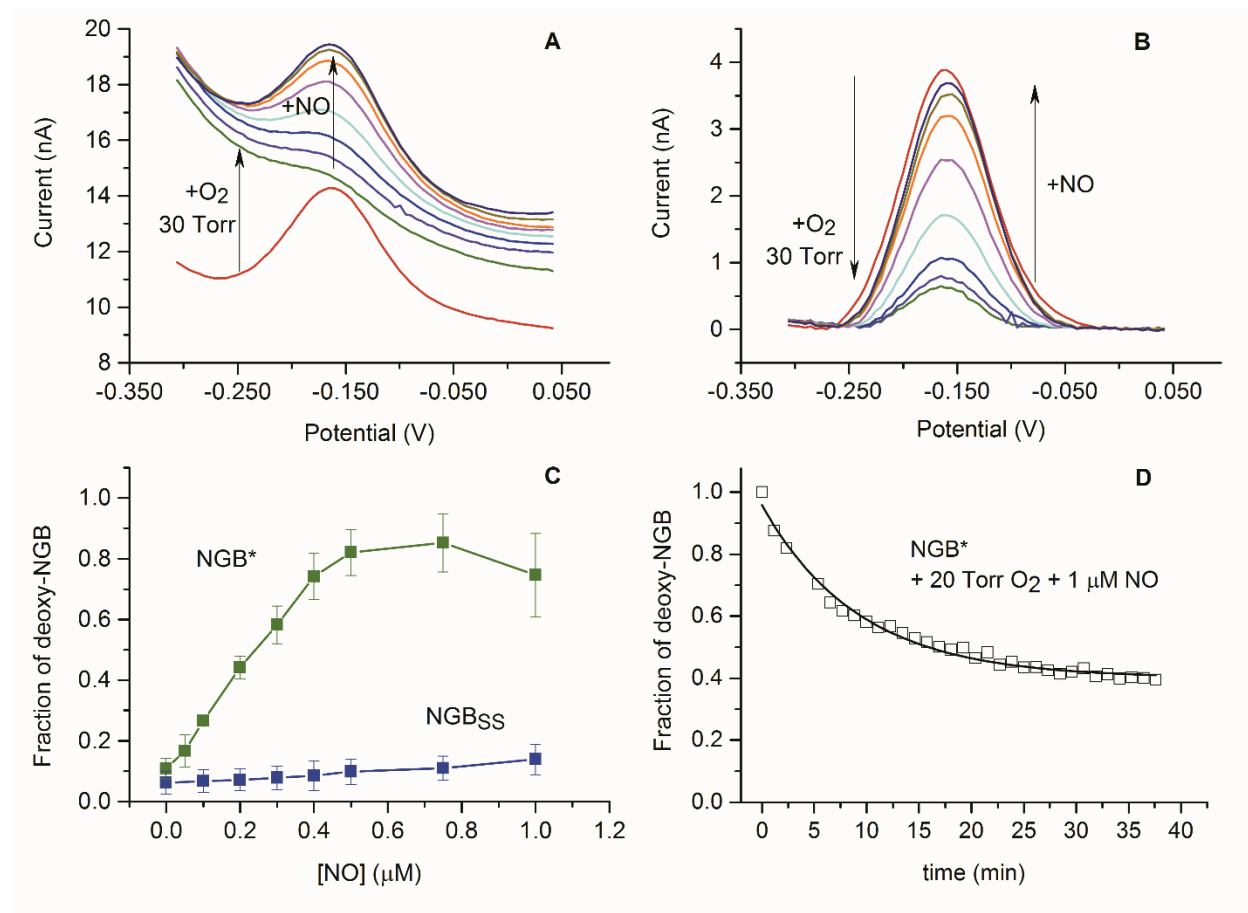
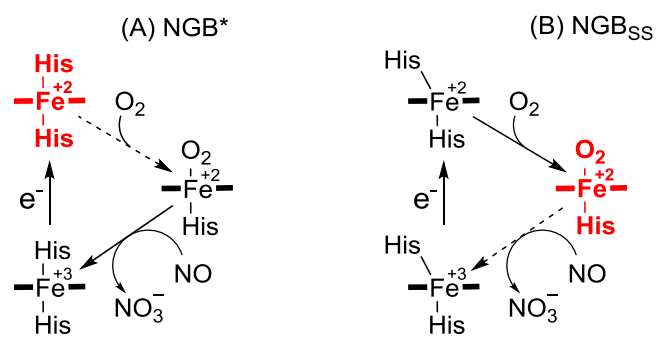


Figure 5.



**Electrochemical evidence for neuroglobin activity on NO at physiological concentrations**

Stanislav Trashin, Mats de Jong, Evi Luyckx, Sylvia Dewilde and Karolien De Wael

*J. Biol. Chem.* published online July 8, 2016

---

Access the most updated version of this article at doi: [10.1074/jbc.M116.730176](https://doi.org/10.1074/jbc.M116.730176)

Alerts:

- [When this article is cited](#)
- [When a correction for this article is posted](#)

[Click here](#) to choose from all of JBC's e-mail alerts

This article cites 0 references, 0 of which can be accessed free at <http://www.jbc.org/content/early/2016/07/08/jbc.M116.730176.full.html#ref-list-1>